

# Superfluid Dynamics within Time-Dependent Density Functional Theory

K. Sekizawa<sup>1,2,3</sup>, A.E. Makowski<sup>4</sup>, A. Barresi<sup>4</sup>, A.M.A. Boulet<sup>4</sup>, P. Magierski<sup>4,5</sup>, G. Wlazłowski<sup>4,5</sup>,  
D.Z. Pećak<sup>4</sup>, M.J. Tylutki<sup>4</sup>, B. Tüzemen<sup>4</sup>, K. Kobuszewski<sup>4</sup>, W. Kragiel<sup>4</sup>, A. Bulgac<sup>5</sup>

<sup>1</sup>Department of Physics, Tokyo Institute of Technology, Japan

<sup>2</sup>Center for Computational Sciences, University of Tsukuba, Japan

<sup>3</sup>RIKEN Nishina Center, Japan

<sup>4</sup>Faculty of Physics, Warsaw University of Technology, Poland

<sup>5</sup>Department of Physics, University of Washington, USA

## Method

We employ Time-Dependent Superfluid Local Density Approximation: TDSLDA

To describe superfluid dynamics in strongly-correlated Fermionic systems, we use **Time-Dependent Density Functional Theory (TDDFT) extended to superfluid systems, known as TDSLDA** [1]. We solve it in 3D uniform grids without symmetry restrictions. Since it requires to solve a huge number ( $10^4$ - $10^6$ ) of 3D, complex, non-linear, coupled PDEs, we do need a supercomputer. With local treatment of pairing, the equations could be solved efficiently on **GPUs**: each thread takes care of each lattice point. With the usage of supercomputers, it has been successfully applied to, e.g., collisions of two superfluid nuclei [2] as well as vortex-nucleus dynamics in the inner crust of neutron stars [3].

**TDSLDA: TDDFT with local treatment of pairing**

Kohn-Sham scheme is extended for non-interacting quasiparticles

► TDSLDA equations (formally equivalent to TDHF or TD-BdG equations)

$$i\hbar \frac{\partial}{\partial t} \begin{pmatrix} u_{k,\uparrow}(\mathbf{r}, t) \\ u_{k,\downarrow}(\mathbf{r}, t) \\ v_{k,\uparrow}(\mathbf{r}, t) \\ v_{k,\downarrow}(\mathbf{r}, t) \end{pmatrix} = \begin{pmatrix} h_{\uparrow\uparrow}(\mathbf{r}, t) & h_{\uparrow\downarrow}(\mathbf{r}, t) & 0 & \Delta(\mathbf{r}, t) \\ h_{\downarrow\uparrow}(\mathbf{r}, t) & h_{\downarrow\downarrow}(\mathbf{r}, t) & -\Delta(\mathbf{r}, t) & 0 \\ 0 & -\Delta^*(\mathbf{r}, t) & -h_{\uparrow\uparrow}^*(\mathbf{r}, t) & -h_{\uparrow\downarrow}^*(\mathbf{r}, t) \\ \Delta^*(\mathbf{r}, t) & 0 & -h_{\downarrow\uparrow}^*(\mathbf{r}, t) & -h_{\downarrow\downarrow}^*(\mathbf{r}, t) \end{pmatrix} \begin{pmatrix} u_{k,\uparrow}(\mathbf{r}, t) \\ u_{k,\downarrow}(\mathbf{r}, t) \\ v_{k,\uparrow}(\mathbf{r}, t) \\ v_{k,\downarrow}(\mathbf{r}, t) \end{pmatrix}$$

$$h_{\sigma} = \frac{\delta E}{\delta n_{\sigma}} : \text{s.p. Hamiltonian}$$

$$\Delta = -\frac{\delta E}{\delta \nu^*} : \text{pairing field}$$

$$n_{\sigma}(\mathbf{r}, t) = \sum_{E_k < E_c} |v_{k,\sigma}(\mathbf{r}, t)|^2 : \text{number density}$$

$$\nu(\mathbf{r}, t) = \sum_{E_k < E_c} u_{k,\uparrow}(\mathbf{r}, t)v_{k,\downarrow}^*(\mathbf{r}, t) : \text{anomalous density}$$

$$\mathbf{j}_{\sigma}(\mathbf{r}, t) = \hbar \sum_{E_k < E_c} \text{Im}[v_{k,\sigma}^*(\mathbf{r}, t)\nabla v_{k,\sigma}(\mathbf{r}, t)] : \text{current}$$

**A large number ( $10^4$ - $10^6$ ) of 3D coupled non-linear PDEs have to be solved!!**  
# of qp orbitals ~ # of grid points

[1] A. Bulgac, Ann. Rev. Nucl. Part. Sci. **63**, 97 (2013);

P. Magierski, Fron. Nucl. Part. Phys. **2**, 57-71 (Bentham Science Publishers 2019).

[2] P. Magierski, K. Sekizawa, and G. Wlazłowski, Phys. Rev. Lett. **119**, 042501 (2017).

[3] G. Wlazłowski, K. Sekizawa, P. Magierski, et al., Phys. Rev. Lett. **117**, 232701 (2016).

## Results (1/2)

We found rapid increases of pairing in fusing magic nuclei

Pairing correlations in nuclear systems are one of the best known characteristics of non-magic atomic nuclei. It implicitly assumes the existence of a pairing phase described by the complex field playing the role of the order parameter. There were only a limited number of attempts to prove other features of pairing in nuclei that are related to the understanding of pairing as a phase.

This allocation extends our previous calculations, reported in [P. Magierski, A. Makowski, M.C. Barton, K. Sekizawa, and G. Wlazłowski, Phys. Rev. C **105**, 064602 (2022)], with realistic nuclear energy density functional. We have performed fully microscopic calculations of magic/doubly-magic nuclear systems. **Figure 2** shows the average pairing gap in logarithmic scale. Four panels, from left to right, present results for  $^{90}\text{Zr}+^{90}\text{Zr}$ ,  $^{90}\text{Zr}+^{132}\text{Sn}$ ,  $^{40}\text{Ca}+^{208}\text{Pb}$ ,  $^{48}\text{Ca}+^{208}\text{Pb}$  reactions. On the horizontal axis, the center of mass energy divided by the dynamical Coulomb barrier for fusion,  $E_{c.m.}/V_B$ , is indicated, where values below present the temperature of the system extracted using the Thomas-Fermi approximation. We found that the appearance of the pairing gap is correlated with elongation of the system. We point out that the rapid growth of the pairing is exponential, which occurs the collision time around 400-500 fm/c. This is due to rapid change of the density of states at the fermi surface.

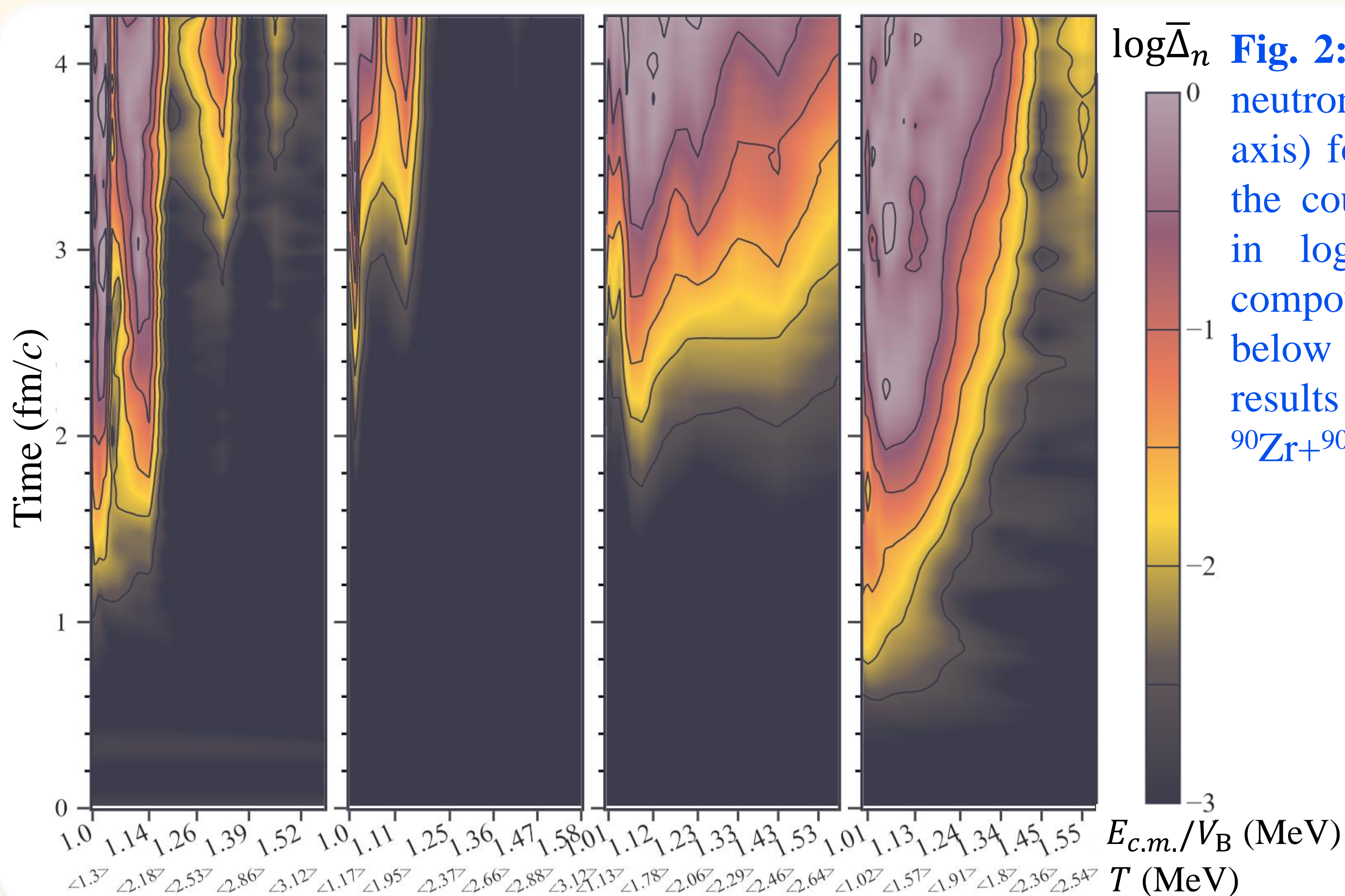


**Fig. 2:** Evolution of the average pairing gap of neutrons is shown as a function of time (vertical axis) for a series of relative collision energy to the coulomb barrier,  $E_{c.m.}/V_B$  (horizontal axis), in logarithmic scale. Temperatures of the compound system after collision is denoted below the energies in MeV. Figure presents results for four systems (from left to right)  $^{90}\text{Zr}+^{90}\text{Zr}$ ,  $^{90}\text{Zr}+^{132}\text{Sn}$ ,  $^{40}\text{Ca}+^{208}\text{Pb}$ ,  $^{48}\text{Ca}+^{208}\text{Pb}$ .



Recent works [B. Tüzemen *et al.*, *New J. Phys.* **25**, 033013 (2023)] have explored the formation of disordered structures in spin-imbalanced unitary Fermi gases, as well as a result of Higgs mode decay in interaction-quenched configurations [A. Barresi, A.M.A. Boulet, G. Wlazłowski, *Sci. Rep.* **13**, 11285 (2023)] (also performed during the previous allocation).

The current allocation has been dedicated to the exploration of such disordered structures at various polarizations in the range  $0.3\% < P < 18\%$  and in the presence of vortex dipoles. Through the use of WSLDA Toolkit's customization, we have simulated a strongly interacting Fermi gas in a  $100 \times 64 \times 16$  lattice in which a position-dependent chemical potential separates two zones: one where polarization is set to 0, where dipoles are imprinted using the same procedure as [Barresi, Boulet, Wlazłowski], and a second one with  $P > 0\%$ , where ferrons (polarized droplets predicted in our preceding study [P. Magierski, B. Tüzemen, and G. Wlazłowski, *Phys. Rev. A* **100**, 033613 (2019)]) and nodal lines are generated. **Figure 1a)** shows an example of such configuration.

TDDFT methods allow us to evolve the configuration in time and study the interactions between moving dipoles and ferronic structures. **Figure 1** shows snapshots from a trajectory where the collision causes the otherwise stable dipole to vanish; the dipole emerges from the collision with reduced size. **Figure 2** shows the ratio between final and initial distance between the vortex cores as a function of initial distance and for different values of global polarization, highlighting the intensity of the dissipation taking place upon collisions.

Further exploration involves the impact of Andreev states in the dynamics of the collision, the role of the impact parameter (or angle of collision) between the dipole and the ferron, and the eventual differences at higher temperatures or in different interaction regimes such as BCS.

A publication is expected to feature the current research in the following months.

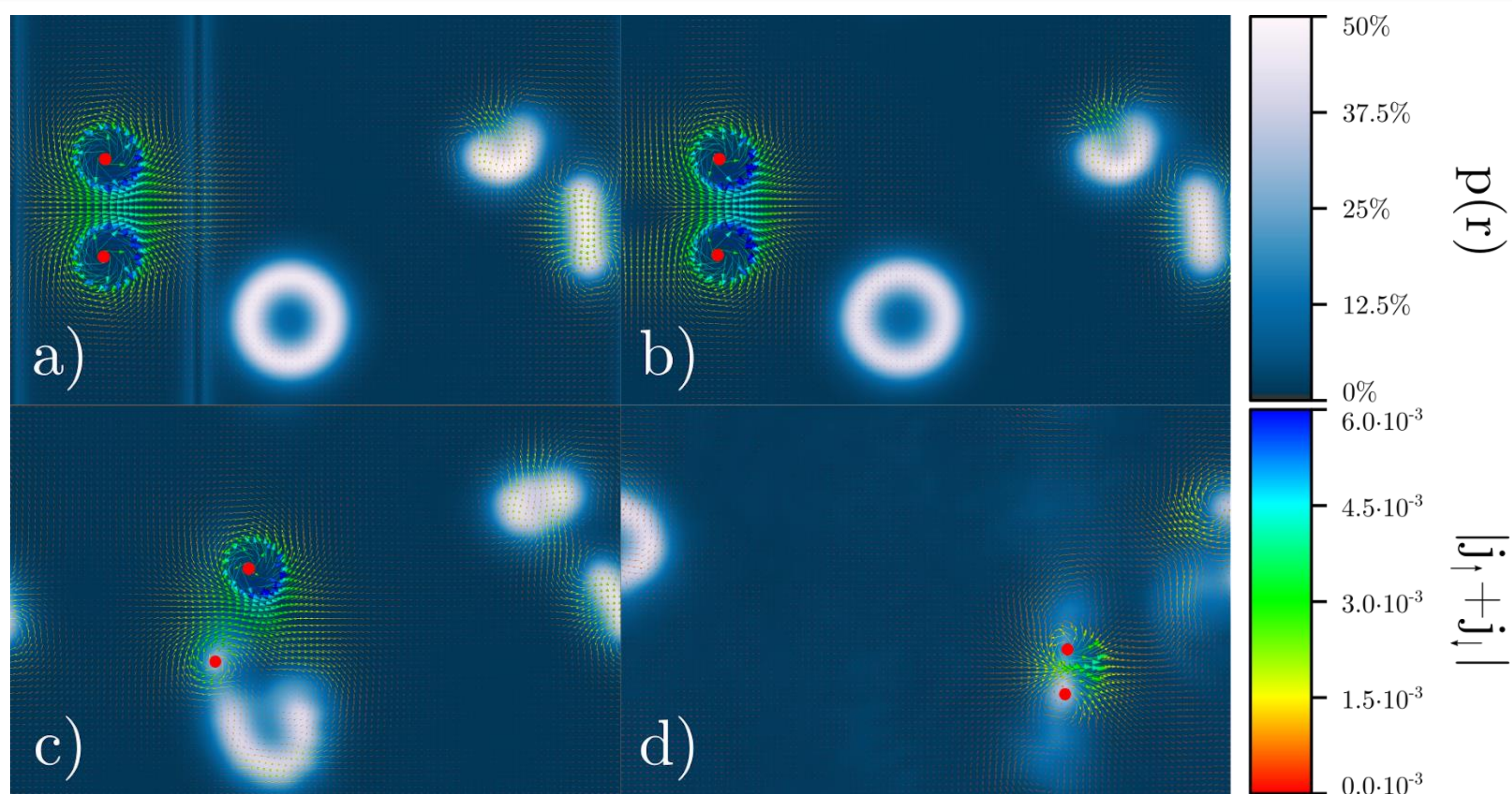


**Fig. 1:** (a) Initial configuration after the vortices are imprinted on the unpolarized section. The two vertical lines are a numerical effect around the section where polarization is kept null. (b) polarization constraints are removed; the dipole starts propagating linearly. (c) Dipole-ferron collision. Notably, part of the unpaired particles become bound inside the closest vortex core. (d) The ferron has been annihilated, whereas the dipole survives with reduced size. Polarization inside the vortex cores is now nonzero, suggesting that Andreev states might play a role in the dissipation.

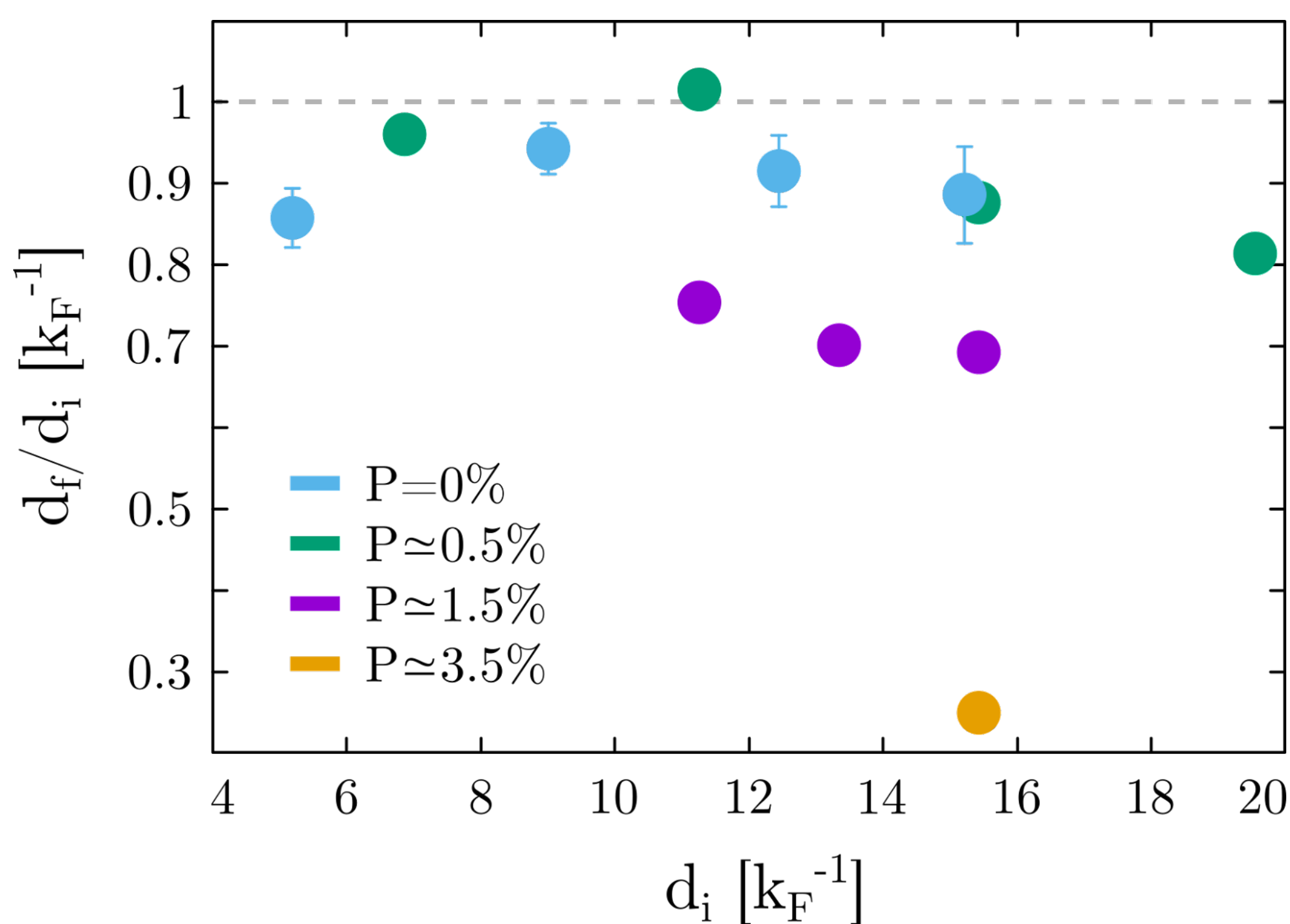


**Fig. 2:** Distance ratio as a function of initial distance. The line at  $d_f/d_i = 1$  indicates the ratio of a dipole propagating in an unpolarized medium without obstacles. Blue dots are taken from [A. Barresi, A.M.A. Boulet, G. Wlazłowski, P. Magierski, *Phys. Rev. Lett.* **130**, 043001 (2023)]. Datasets for  $P > 3\%$  resulted in dipole annihilation ( $d_f/d_i = 0$ ) with a single exception (orange dot).